



Numerical solution of the 3D time dependent Schrödinger equation in spherical coordinates: Spectral basis and effects of split-operator technique

Tor Sørøvik^{a,*}, Tore Birkeland^a, Gabriel Okša^b

^a Department of Mathematics, University of Bergen, Norway

^b Department of Informatics, Institute of Mathematics, Slovak Academy of Sciences, Slovakia

ARTICLE INFO

Article history:

Received 8 November 2007

Received in revised form 29 May 2008

MSC:

65M70

81V45

Keywords:

The time dependent Schrödinger equation

Split step

Spectral approximation

Variable transformation

ABSTRACT

We study a numerical solution of the multi-dimensional time dependent Schrödinger equation using a split-operator technique for time stepping and a spectral approximation in the spatial coordinates. We are particularly interested in systems with near spherical symmetries. One expects these problems to be most efficiently computed in spherical coordinates as a coarse grain discretization should be sufficient in the angular directions. However, in this coordinate system the standard Fourier basis does not provide a good basis set in the radial direction. Here, we suggest an alternative basis set based on Chebyshev polynomials and a variable transformation.

Furthermore, it is shown how the use of operator splitting produces a splitting error which introduces high frequency modes in the numerical solution in the case of the singular Coulomb potential. Incorporating the Coulomb potential into the radial Laplacian provides a much better splitting. Fortunately our new basis set allows this in some cases.

Numerical experiments are presented which demonstrate the advantages and limitations of our technique. Details are demonstrated by 1D toy examples, while the superior efficiency is demonstrated by a 3D example.

© 2008 Elsevier B.V. All rights reserved.

1. Introduction

A popular technique for solving the Time Dependent Schrödinger Equation (TDSE) is to use a split-operator technique [4, 7]. In this approach the equation is split into a number of simpler equations to be solved in a given sequential order. By doing so we do no longer solve the original system (unless the operators commute), but a (hopefully) closely related system. However, this nearby system may have special features not present in the original system and thus the split-operator solution may exhibit behaviour not representative of the true solution. In Section 4 we discuss when and why this happens. We also explain how the problem can be circumvented by taking care in the splitting.

For solving each of the equations in the split-operator formulation one may use a spectral approximation in space. This technique becomes particularly easy and elegant when the choice of basis functions equals the eigenfunctions of the corresponding (partial) operators. In many cases projections onto spaces spanned by a relative small set of eigenfunctions also provide good spectral approximation to the wave function, but not always. One important exception is when spherical coordinates are used. In the radial direction the operator becomes the 1D Laplacian. To obtain the necessary accuracy in the radial direction using a Fourier basis, one typically needs orders of magnitude more points in this direction than in the angular directions.

* Corresponding address: Department of Mathematics, University of Bergen, Johannes Brunsgt. 12, 5008 Bergen, Norway. Tel.: +47 55584172.
E-mail address: tor.sorevik@math.uib.no (T. Sørøvik).

This problem is addressed by doing a detailed study in 1D. Our approach is to use a transformation of variable in the radial direction and to apply Chebyshev approximation to the transformed equation.

The reminder of this introduction is used to give the necessary background, outline the computational technique, and point out the problem which may occur when using a Fourier basis.

1.1. Operator splitting

The TDSE may be written

$$i\frac{\partial}{\partial t}\Psi(\mathbf{x}, t) = H\Psi(\mathbf{x}, t); \quad \mathbf{x} \in \mathbb{R}^N; t \geq 0. \quad (1)$$

The Hamiltonian operator is $H = \nabla^2 + V(\mathbf{x}, t)$ where ∇^2 represents the kinetic energy and V represents the potential energy.

In hyperspherical coordinates the Laplacian takes the form¹:

$$\nabla^2 = -\frac{1}{2} \left(\frac{\partial^2}{\partial r^2} + \frac{N-1}{r} \frac{\partial}{\partial r} - \frac{\Lambda^2(N)}{r^2} \right). \quad (2)$$

$\Lambda^2(N)$ is the grand angular momentum operator and represents the action of the Laplacian in all angular directions. It has the set of hyperspherical harmonics, $\mathcal{Y}_{\ell}(\Omega_{N-1})$ as an orthogonal set of eigenfunctions. For simplicity in the notation, we will restrict ourselves to $N = 3$, for the remainder of this paper. For $N = 3$ the hyperspherical harmonics reduce to the familiar spherical harmonics $Y_m^l(\Omega)$.

An underlying assumption for this work is that our wave function is smooth and well-behaved in all angular directions, and consequently can be accurately approximated with a small set of eigenfunctions, while this is not the case in the radial direction. A computational advantage of spherical coordinates is that the domain becomes bounded and periodic in the angular directions, and we only need to deal with an unbounded domain in the radial direction.

A standard trick is to remove the first derivative term by introducing the reduced wave function $\Phi = r^{(N-1)/2}\Psi$.

We intend to solve (1) in spherical coordinates with the kinetic energy given by (2). The effect of the potential operator is easily computed in coordinate space, while the effect of the Laplacian operator may be effectively and accurately computed in spectral space. This observation indicates that operator splitting (or the fractional step method) could be a good solution strategy. We do a 3-way symmetric Strang splitting [13] of the Hamiltonian, and take as our partial operators: the radial Laplacian ($\frac{\partial^2}{2\partial r^2}$), the angular momentum operator ($\frac{-\Lambda^2(N)}{2r^2}$) and the potential operator ($V(r, \Omega, t)$).

Advancing the solution from t_n to $t_{n+1} = t_n + \Delta t$ can be described in terms of the operator exponential as

$$\Phi(r, \Omega, t_{n+1}) = e^{\frac{i\Delta t}{4} \frac{\partial^2}{\partial r^2}} e^{\frac{-i\Lambda^2(N)\Delta t}{4r^2}} e^{-iV(r, \Omega, \Delta t)} e^{\frac{-i\Lambda^2(N)\Delta t}{4r^2}} e^{\frac{i\Delta t}{4} \frac{\partial^2}{\partial r^2}} \Phi(r, \Omega, t_n) + O(\Delta t^3). \quad (3)$$

To compute this one needs to solve, in the given sequential order, the following equations with their associated initial values:

$$\frac{\partial}{\partial t} \Phi^* = \frac{i}{2} \frac{\partial^2}{\partial r^2} \Phi^*; \quad \Phi^*(t_n) = \Phi(r, \Omega, t_n) \quad (4)$$

$$\frac{\partial}{\partial t} \hat{\Phi} = \frac{-i\Lambda^2}{2r^2} \hat{\Phi}; \quad \hat{\Phi}(t_n) = \Phi^*(t_{n+1/2}) \quad (5)$$

$$\frac{\partial}{\partial t} \tilde{\Phi} = -iV\tilde{\Phi}; \quad \tilde{\Phi}(t_n) = \hat{\Phi}(t_{n+1}) \quad (6)$$

$$\frac{\partial}{\partial t} \hat{\Phi} = \frac{-i\Lambda^2}{2r^2} \hat{\Phi}; \quad \hat{\Phi}(t_n + \Delta t/2) = \tilde{\Phi}(t_{n+1}) \quad (7)$$

$$\frac{\partial}{\partial t} \Phi^* = \frac{i}{2} \frac{\partial^2}{\partial r^2} \Phi^*; \quad \Phi^*(t_n + \Delta t/2) = \hat{\Phi}(t_{n+1}) \quad (8)$$

$$\Phi(r, \Omega, t_{n+1}) = \Phi^*(t_{n+1}). \quad (9)$$

For this splitting scheme the global error is known to be $O(\Delta t^2)$. Higher order, more sophisticated splitting schemes do exist, but will not be considered in this paper. See [16] on how to construct such methods. For a thorough review of splitting techniques see [10]. [11] applies high-order splitting to the non-linear 1D Schrödinger equation.

¹ Throughout this paper we use atomic units; $\hbar = m = 1$.

1.2. Spectral basis functions

The solution to each of these equations can formally be written as

$$\Phi(r, \Omega, t + \Delta t) = e^{A\Delta t} \Phi(r, \Omega, t), \quad (10)$$

where A represents any time independent operator. Computing this becomes easy whenever the operator is diagonal. The potential operator is diagonalized by the grid representation, while the two other operators need to have Φ to be projected onto a space spanned by the orthogonal set of eigenfunctions of the operator. As an example, in 3 dimension the eigenfunctions of $\Delta^2(3)$ are the set of spherical harmonic functions, $Y_m^l(\Omega)$ with eigenvalues $l(l+1)$. Thus by expanding

$$\Phi(r, \Omega, t) = \sum_{l=0}^{L_{\max}} \sum_{m=-l}^l c_{lm}(r, t) Y_m^l(\Omega) \quad (11)$$

the effect of applying the operator $\frac{-iA^2(3)}{2r^2}$ simply becomes

$$\Phi(r, \Omega, t + \Delta t) = \sum_{l=0}^{L_{\max}} \sum_{m=-l}^l \hat{c}_{lm} Y_m^l(\Omega), \quad (12)$$

where

$$\hat{c}_{lm}(r, t) = e^{\frac{-il(l+1)\Delta t}{2r^2}} c_{lm}(r, t). \quad (13)$$

A similar technique can be used for advancing Eq. (4) in time. The eigenfunctions of the 1D Laplacian on a bounded interval $[-R, R]$ are the celebrated Fourier functions $e^{\frac{i\pi k r}{R}}$ with eigenvalues $-\left(\frac{\pi k}{R}\right)^2$. However, in our case this requires us to truncate the computational domain from $[0, \infty)$ to a finite domain, say $[0, R]$. On this domain the periodic extension of the wave function could not be expected to be a smooth function, and consequently the convergence of the Fourier expansion could be painfully slow [8]. The situation may be improved by symmetrizing our function and domain by defining

$$\bar{\Phi}(r, \Omega, t) = \begin{cases} \Phi(r, \Omega, t); & 0 \leq r \leq R \\ -\Phi(-r, \Omega, t); & -R \leq r < 0. \end{cases} \quad (14)$$

The limitation of this trick hinges on the smoothness of $\bar{\Phi}(r, \Omega, t)$ at the origin. In the case where Φ behaves as re^{-r^2} , $\bar{\Phi}$ is smooth and the technique works well, while if Φ is of the form re^{-r} , the second derivative of $\bar{\Phi}$ becomes discontinuous and the convergence correspondingly slow.

A large number of expansion functions corresponds to a large number of radial evaluation points. Thus the total cost of computation may become prohibitively expensive. Various techniques have been suggested for reducing the number of radial evaluation points.

Fattal et al. [3] suggested complementing the technique described above with a variable transformation $r = x - A \tan^{-1}(\beta x) = f(x)$ for some constant A and β . In this new variable the second-order derivative for $r = x = 0$ becomes

$$\Phi_{xx}(0) = (f_x(0))^2 \Phi_{rr}(0). \quad (15)$$

Thus the non-smoothness at the origin can be countered by having $f_x(0)$ sufficiently small, which is achieved for their transformation provided $A\beta = 1$.

Boyd et al. [2] took another path. They avoided the inherited problems with the Fourier basis functions by replacing them with orthogonal basis functions defined on the interval $[0, \infty)$. They suggested using either Laguerre functions or rational Chebyshev functions, and showed the efficiency and accuracy of this approach for the eigenvalue problem of the time independent Schrödinger equation.

In this paper we suggest and test an approach based on variable transformation, as in [3]. However, we do not artificially extend our interval to negative r , nor do we apply cut-off. As a result we do not expect the periodic extension of our function to be smooth, and consequently we apply a Chebyshev spectral approximation in space. Our technique is related to one presented by Wang, Chu and Laughlin [14]. However, they used Legendre polynomials as basis functions and did not play with different transformations. They also used cut-off of the original interval before introducing variable transformation, as well as yet another transformation to the wavefunction to symmetrize the operator. In [5] the same technique is extended for computation in hyperspherical coordinates in 6D.

A common observation is that the Coulomb potential gives rise to unphysical high frequent oscillation in the numerical solution near the origin. In Section 4 we describe the nature of these oscillations and demonstrate how our new discretization scheme gives us a handle for dealing with this problem. But first we describe the variable transformations in Section 2. A scheme for the time propagation of the 1D Laplacian when a Chebyshev expansion is used, is developed in Section 3. In Section 5 we demonstrate the accuracy and efficiency by numerical examples.

Table 1

The 3 tested transformations and some of their properties

No.	$x(r)$	$x'(r)$	$x''(r)$	The inverse
1	$x(r) = \frac{L_1 - r}{L_1 + r}$	$x'(r) = \frac{-2L_1}{(L_1 + r)^2}$	$x''(r) = \frac{4L_1}{(L_1 + r)^3}$	$r(x) = L_1 \frac{1-x}{1+x}$
2	$x(r) = \frac{4}{\pi} \tan^{-1} \frac{r}{L_2} - 1$	$x'(r) = \frac{4L_2}{\pi(L_2^2 + r^2)}$	$x''(r) = -\frac{8L_2 r}{\pi(L_2^2 + r^2)^2}$	$r(x) = L_2 \tan(\frac{\pi}{4}(x+1))$
3	$x(r) = 1 - 2e^{-r/L_3}$	$x'(r) = \frac{2}{L_3} e^{-r/L_3}$	$x''(r) = -\frac{2}{L_3^2} e^{-r/L_3}$	$r(x) = -L_3 \ln \frac{1-x}{2}$

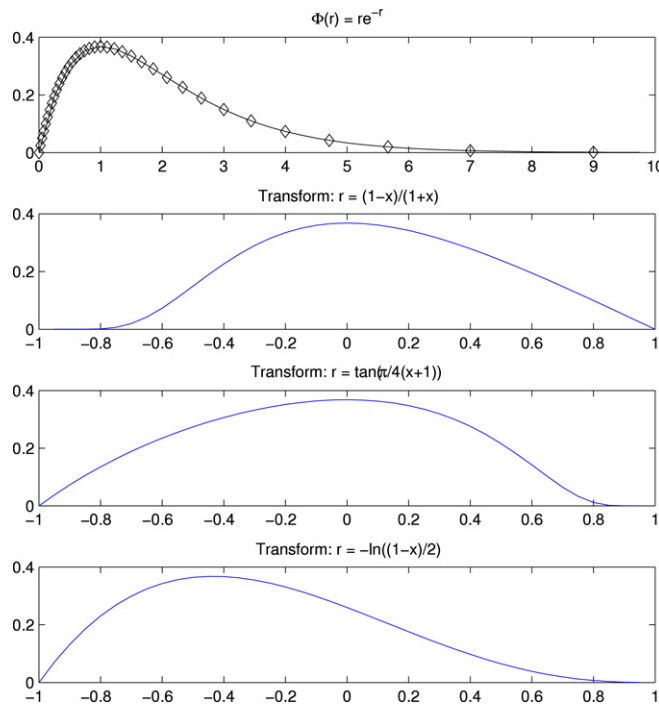


Fig. 1. This figure shows how the different transformations transform $\Phi_1(r) = re^{-r}$; $r \in [0, \infty)$. Here $L_1 = L_2 = 1$ while $L_3 = 3$. The top figure displays $\Phi_1(r)$. The diamonds display the Chebyshev collocation points after being transformed by (17).

2. Change of variable

With a change of variable $x(r)$ the radial Laplacian becomes:

$$\frac{\partial^2}{\partial^2 r} \Phi(x(r)) = \frac{\partial^2}{\partial^2 x} \Phi(x(r)) \left(\frac{\partial x}{\partial r} \right)^2 + \frac{\partial}{\partial x} \Phi(x(r)) \frac{\partial^2 x}{\partial r^2}. \quad (16)$$

2.1. The variable transforms

We are interested in a transformation which takes $x(r)$ onto $[-1, 1]$ or $(-1, 1]$ for $r \in [0, \infty)$. There is an infinite number of such transformations. We have modified 3 transformations given by Boyd in [1]. In [1] these are for $r \in (-\infty, \infty)$. With simple modifications they become:

$$x(r) = \frac{L_1 - r}{L_1 + r}; \quad r \in [0, \infty); \quad x \in (-1, 1], \quad (17)$$

$$x(r) = \frac{4}{\pi} \tan^{-1} \left(\frac{r}{L_2} \right) - 1; \quad r \in [0, \infty); \quad x \in [-1, 1), \quad (18)$$

$$x(r) = 1 - 2e^{-r/L_3}; \quad r \in [0, \infty); \quad x \in [-1, 1). \quad (19)$$

Some basic properties of these transformations are given in Table 1. The constants L_1 , L_2 , and L_3 can be chosen to strengthen or weaken the transform as needed.

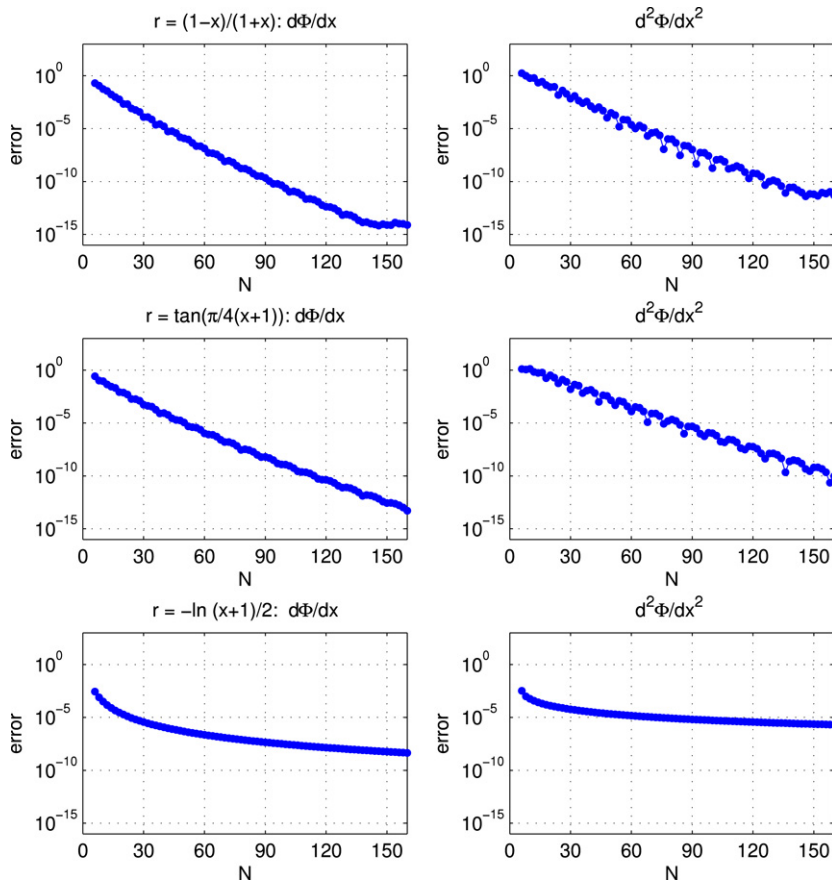


Fig. 2. The error of the Chebyshev approximation to 1st and 2nd derivative of $\Phi_1(r)$ when the 3 transformations are applied. N is the number of collocation points.

In Fig. 1 we illustrate the effect of these transformations on $\Phi(r) = re^{-r}$, the ground state of the Coulomb problem in 3D with no angular dependency. Φ is still bounded and homogeneous, but exists on the semi-open intervals $(-1, 1]$ or $[-1, 1)$. However, it does not have a smooth periodic extension, and consequently we do not expect a Fourier expansion to converge rapidly. Moreover the eigenfunctions of the transformed operator are no longer the Fourier functions. Thus the very reason for approximating $\Phi(x)$ by a Fourier expansion is not present anymore. We follow conventional wisdom and use the Chebyshev polynomials for spectral approximation of non-periodic functions on a bounded interval.

In Fig. 2 we display the error when approximating the first and second derivatives of $\Phi_1(r) = re^{-r}$ with respect to x , for the different transformations (17)–(19).

It is evident from Fig. 2 that we obtain geometrical convergence with the Chebyshev approximation for the first two transformations, but not for the third one, when applied to the Coulomb ground state function.

3. Time propagation of the Laplacian

Inserting (16) into Eq. (4) and discretizing with Chebyshev collocation method give us the following linear discrete system

$$\frac{\partial}{\partial t} \mathbf{u}(t) = -\frac{i}{4} A \mathbf{u}(t), \quad (20)$$

where $\mathbf{u}(t)$ is the vector approximating $\Phi(r)$ at the Chebyshev collocation points $x_j = \cos(\frac{j\pi}{N})$; $j = 0, \dots, N$. The matrix A is

$$A = X^2 D^2 + YD. \quad (21)$$

Here D is the $(N+1) \times (N+1)$ Chebyshev differentiation matrix while X is the diagonal matrix with entries $(X)_{ii} = \frac{\partial x}{\partial r}(r_i)$

and Y the diagonal matrix with entries $(Y)_{ii} = \frac{\partial^2 x}{\partial r^2}(r_i)$.

In our case we have the boundary values

$$\Phi(r=0) = \Phi(r \rightarrow \infty) = 0 \quad (22)$$

implying $u_0(t) = u_N(t) = 0; \forall t$. Thus the first and last columns of D do not contribute to anything in the matrix–vector product Au , nor are we interested in the first and last entries of the result vector. Thus we can restrict the computation to the matrices:

$$\hat{D} = D(1 : N - 1, 1 : N - 1); \quad \text{and} \quad \tilde{D} = D^2(1 : N - 1, 1 : N - 1) \quad (23)$$

and similarly for X and Y . This not only saves time and space in the computation, but more importantly it avoids the endpoint singularity of X and Y .

A is not symmetric, nor is it a normal matrix. However, it is the discrete counterpart of a self-adjoint operator, and an affine scaling of the axis should not alter the fundamental properties of our operator, nor should the discretization of the operator. Thus for (20) to faithfully represent the physics, A must have purely real eigenvalues. Numerical computations have confirmed that this is indeed the fact.

A solution to (20) can now be obtained by computing the eigendecomposition of $A = R\Lambda R^{-1}$, and substituting $y = R^{-1}u$. With this substitution the system of equations diagonalize and is easily solved in $O(N)$ operation. The cost will be $O(N^3)$ for computing the eigendecomposition, but this only needs to be done once at the beginning. Then, in each time step one needs to recover $u = Ry$ at a cost of $O(N^2)$.

Alternatively we can solve (20) by a numerical technique. By not explicitly forming A the matrix–vector multiplication involved can be performed in $O(N \log N)$ as the effect of D can be computed by an FFT. We have not pursued this possibility, as our focus is on producing a minimal basis set only. Remember, where this is of importance is for higher-dimensional problems. Here the most expensive operation is to do the (hyper)spherical transformations in the angular directions. A saving in radial collocation points then translates into a saving in the number of (hyper)spheres.

4. The splitting error

For splitting into 2 linear operators A and B , standard error analysis of splitting methods [10] gives the following formula for the local error of the Strang splitting

$$E(r, \Delta t) = e^{(A+B)\Delta t} \Phi(r, t) - e^{A\Delta t/2} e^{B\Delta t} e^{A\Delta t/2} \Phi(r, t) \quad (24)$$

$$= ([A, [A, B]] + 2[B, [B, A]]) \Delta t^3 + O(\Delta t^5) \Phi(r, t). \quad (25)$$

The commutator expression in the bracket in front of the Δt^3 -term will in our case produce a function of the spatial variables. The form of this function appears to be crucial for the accuracy.

We illustrate this by taking a closer look at two canonical cases in 3D. To simplify the computation and highlight the crucial point, we assume full angular symmetry. Then the angular dependency and operator disappear and we are left with one spatial degree of freedom, the radial one. Below we consider the ground states of two canonical cases, the Coulomb potential $V_1(r) = -1/r - 0.5$ and the harmonic oscillator $V_2(r) = 2r^2 - 4$. Both potentials have been scaled to yield ground state energy $E_0 = 1$. These potentials correspond to the following solutions:

$$\Phi_1(r, t) = re^{-r} e^{it}, \quad (26)$$

$$\Phi_2(r, t) = re^{-r^2} e^{it}. \quad (27)$$

Applying (25) we obtain the following leading terms in the one-step error

$$E_1(r, \Delta t) = -\frac{i\Delta t^3}{12r^3} \Phi_1(r, t) + O(\Delta t^5), \quad (28)$$

$$E_2(r, \Delta t) = -\frac{i\Delta t^3}{3} P_8(r) \Phi_2(r, t) + O(\Delta t^5). \quad (29)$$

Here $P_8(r)$ is a polynomial of degree 8. These error functions are of fundamentally different nature. $|E_2(r, \Delta t)|$ takes its maximum for $r \approx 1$, and the grid point corresponding to the maximum error is more or less independent of N .

However, $E_1(r, \Delta t)$ has a singularity at the origin. Since we omit $r_0 = 0$, the collocation point contributing to the largest error is

$$x_1 = \cos\left(\frac{\pi}{N}\right) \Rightarrow r_1 = r(x_1) \approx \left(\frac{\pi}{N}\right)^2. \quad (30)$$

Thus increasing N to obtain a better spectral accuracy, will have a disastrous effect on the splitting error. This might be countered by reducing Δt , but note that just to keep splitting error constant an increasing in N by a factor c needs to be countered by a reduction of the time step with a factor c^2 .

Fig. 3 illustrates what happens. The top and the bottom frames show nice spectral convergence rate for $\Phi(r, 0)$ and $\Phi(r, \Delta t)$ respectively. The middle frame demonstrates how all high frequencies have been corrupted by noise as the first time propagation by the potential operator is applied. When first introduced this noise never disappears.

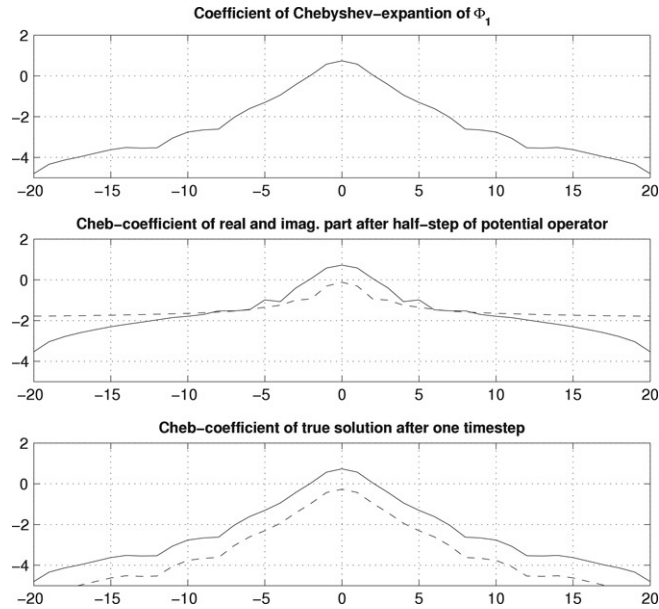


Fig. 3. The Chebyshev expansion coefficients for Φ_1 . Top: the initial value, middle: after a halfstep by the potential operator, $\Delta t = 0.1$. Bottom: The true solution after a full step ($\Delta t = 0.1$). $N = 40$. The solid line represents the real part while the dashed one represents the imaginary part.

An alternative understanding of the splitting error is offered by comparing the exact solution of the original system to the exact solution of (4)–(8). For the Coulomb potential the coefficient in the full equation has a singularity for $r = 0$, while the solution $\Phi(r, t)$ is nice and smooth also for $r = 0$. This does of course imply that the singular coefficient is countered by $\Phi(r) \rightarrow 0$ as $r \rightarrow 0$ such that the term $V_1(r)\Phi(r)$ is well defined for $r = 0$. It is crucial for a splitting that the partial solutions too have this property. But this is not the case with our splitting.

Again, assuming angular symmetry we can omit (5) and (7) from our computation. The radial Laplacian operator behaves as a diffusion operator and thus a smooth solution only becomes smoother. For time independent potential, (6) can be solved exactly, and having discretized in space we obtain

$$\tilde{\Phi}(r_i, t_{n+1}) = e^{-iV(r_i)\Delta t} \Phi^*(r_i, t_{n+0.5}), \quad (31)$$

which for $V_1(r)$, causes extremely fast oscillations in $\tilde{\Phi}(r_i, t_{n+1})$ near the singularity at $r = 0$. These oscillations are not present in the true solution of (27) and will not be sufficiently smoothed by the next partial step. Note that misinterpreting these oscillations as insufficient spectral resolution and trying to cure the problem by increasing the number of radial evaluation points, actually make things worse!

Of course, for these simple examples there is no reason to do any splitting at all. One should simply extend the matrix A of (21) by an extra term representing the discrete potential operator, whenever that is possible. The advantage of this is convincingly demonstrated by the experiments in the next section.

5. Numerical experiments

5.1. Only radial dependency

We have tested our technique with the two simple, fully symmetric problems without angular dependencies, introduced above.

In Table 2 we summarise the results when applying our scheme to the harmonic oscillator, $\Phi_2(r, t)$, using a spectral resolution of $N = 40$. We notice that the error is independent of the transformation used and is proportional to $O(\Delta t^2)$, which indicate that the spectral approximation error is too small to be seen, regardless of the time step and transformation used. Thus the error is a function of the splitting error only.

This suspicion is confirmed by a second test where we keep the time step fixed and change the number of collocation points. This is illustrated in Fig. 4.

Here $\Delta t = 0.005$. Using a very coarse grid the spatial error dominates but improves with spectral accuracy as we increase N . When the total error becomes approximately 1.7×10^{-5} , the splitting error dominates and no improvement is seen as we reduce the spatial approximation error by further increasing N .

Applying the same two tests to the Coulomb problem, $\Phi_1(r, t)$, gives a completely different picture. After only one time step the numerical solution is contaminated by noise. High frequencies, not present in the true solution, are introduced.

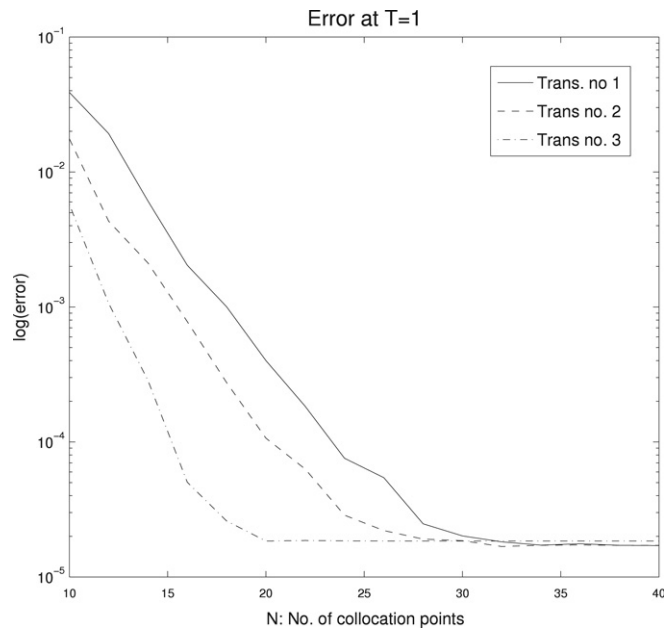


Fig. 4. The error in $\Phi_2(r, 1)$, as a function of the spatial resolution, when using $\Delta t = 0.005$.

Table 2

The error, in L_2 -norm, for the 3 different transformations when computing $\Phi_2(r, T = 1)$, with a different time step

Δt	$x(r) = \frac{1-r}{1+r}$	$x(r) = \frac{\pi}{4} \tan^{-1} r - 1$	$x(r) = 1 - 2e^{-r/3}$
.1	6.4619e-03	6.4800e-03	6.8131e-03
.05	1.6130e-03	1.6175e-03	1.7001e-03
.025	4.0308e-04	4.0421e-04	4.2482e-04
.0125	1.0074e-04	1.0104e-04	1.0619e-04
.00625	2.5161e-05	2.5252e-05	2.6548e-05
.003125	6.2695e-06	6.3073e-06	6.6369e-06

The spectral resolution is $N = 40$ collocation points.

Table 3

Error in the numerical computation of $\Phi_1(r, 1)$ as a function of $(N, \Delta t)$

N	.1	.05	.025	.0125	.00625	.003125	.0015625	.00078125
10	5.24e-02	4.37e-02	3.05e-03	9.48e-03	1.16e-02	1.94e-03	1.77e-03	1.80e-03
12	6.25e-01	4.11e-01	1.66e-01	6.35e-03	7.35e-03	7.11e-03	1.51e-03	1.45e-03
14	2.20e-01	4.49e-01	4.41e-01	4.69e-01	1.47e-03	1.72e-03	1.57e-03	3.77e-04
16	1.24e-01	8.00e-02	1.56e-02	1.58e-02	8.03e-03	1.98e-03	2.63e-04	2.71e-04
18	1.02e-01	6.74e-02	7.13e-02	8.42e-02	2.39e-03	3.10e-03	3.54e-04	6.28e-04
20	8.90e-02	5.66e-02	2.17e-02	3.67e-03	6.45e-03	1.35e-03	7.67e-04	7.99e-04
22	1.05e-01	4.93e-02	2.47e-02	4.29e-02	2.25e-03	2.42e-03	2.12e-03	3.02e-04

Propagating further in time does not increase the noise level, nor reduces it. Small improvements are seen when decreasing the time step.

The obvious answer to the problems illustrated in Table 3 is to avoid the splitting. As discussed in Section 4, for these simple examples the splitting can be avoided by adding an extra diagonal term representing the potential, to our matrix A . In Fig. 5 we show the results of the same computation using this “nosplit” routine. With no splitting error present anymore we can essentially compute the solution to whatever accuracy we want at an acceptable cost.

We conclude this little 1D exercise with claiming that our spectral approximations do obtain a very good spatial resolution for a closed system with time independent potential. However, the splitting technique may introduce high frequent modes as white noise in intermediate steps, which will corrupt the entire computation. Care must be taken when doing this sort of splitting, and if possible it should be omitted. Contrary to the standard technique we do *not* require our basis functions to be eigenfunctions of the associated partial operators. This gives us greater freedom in how to split the operator. Taking advantage of this is important.

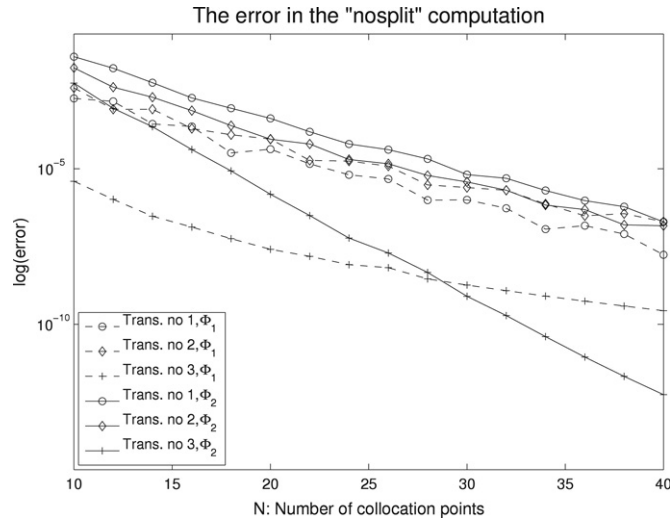


Fig. 5. The error in $\Phi_2(r, 1)$, (solid lines) and $\Phi_1(r, 1)$ (dashed lines) as a function of spatial resolution, using the “nosplit” technique.

5.1.1. Free wavepacket propagation

Our collocation points are focused near the origin and designed to work well for wave functions which stay concentrated near the origin. If that is not the case we may have trouble.

Consider the 1D TDSE with $V = 0$, and the initial condition

$$\Psi(x, 0) = \left(\frac{2}{\pi\sigma}\right)^{1/4} e^{-x^2/\sigma + ik_0 x}. \quad (32)$$

This system corresponds to a free wavepacket with a fixed momentum. On an unbounded domain, the solution will be a diffusive translating wavepacket

$$\Psi(x, t) = \left(\frac{2\sigma}{\pi(\sigma + 2it)^2}\right)^{1/4} e^{-(x-k_0 t)^2/(\sigma + 2it) + ik_0(x-k_0 t) + ik_0^2 t/2}; \quad x \in \mathbb{R}. \quad (33)$$

For this computation we have used the standard transformations, mapping $(-\infty, \infty)$ onto $[-1, 1]$ as they are given in Boyd [1].

In Fig. 6 we display how the error develops as a function of time for different parameter sets and schemes. For a fixed number of points the point density is regulated by the “tuning parameter”, L_i , for the Chebyshev basis and with the cut-off radius for the Fourier basis.

As expected for oscillating functions, when a certain resolution is obtained the Fourier basis provides a very accurate spectral resolution and the computation becomes extremely accurate. However, if the high resolution is obtained by using a too narrow interval, the wavepacket will sooner or later spread beyond this limit and serious error occurs (the case: $N = 200$ and $X_{\max} = 40$). Increasing X_{\max} , the size of the computational domain, while keeping N , the number of grid points, constant, gives insufficient resolution and the computation becomes disastrously wrong. However, keeping the grid resolution fixed when increasing X_{\max} gives near perfect results.

The same balance between sufficient resolution and points far enough from the origin needs to be found for accurate computation with the Chebyshev basis as well. As seen in the top frame of Fig. 1 the collocation points are clustered near the origin. The parameter L_i might be used for stretching them out over a wider interval, but their relative density remains the same. Thus for sufficient resolution at the far end, a large number of points and large L_i are needed.

Taking into account that working with Fourier basis is more economic per evaluation point, we conclude that the Fourier basis is far better for propagating the free wavepacket than any of the transformed Chebyshev bases. This is likely to always be the case for an expanding system. An adaptive or moving grid might be the answer to this problem.

5.2. Full 3D experiments

The real benefit of reducing the number of radial basis functions is of course in true high-dimensional problems.

Now we will demonstrate the scheme on a 3D problem, namely that of finding the ground state energy of H_2^+ .

If we align the H_2^+ molecule along the z -axis, the Hamiltonian for the system can be written as

$$H_{H_2^+} = -\frac{1}{2} \frac{\partial^2}{\partial r^2} + \frac{\Lambda^2}{2r^2} - \frac{1}{\sqrt{(R/2)^2 + r^2 - Rr \cos \theta}} - \frac{1}{\sqrt{(R/2)^2 + r^2 + Rr \cos \theta}}. \quad (34)$$

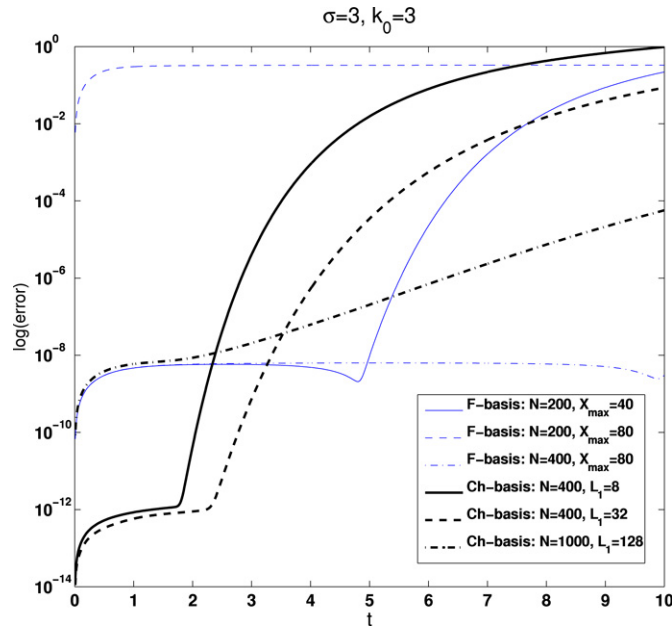


Fig. 6. The error in the free wavepacket propagation as a function of t : thin lines for Fourier basis; thick lines for Chebyshev+transformed basis.

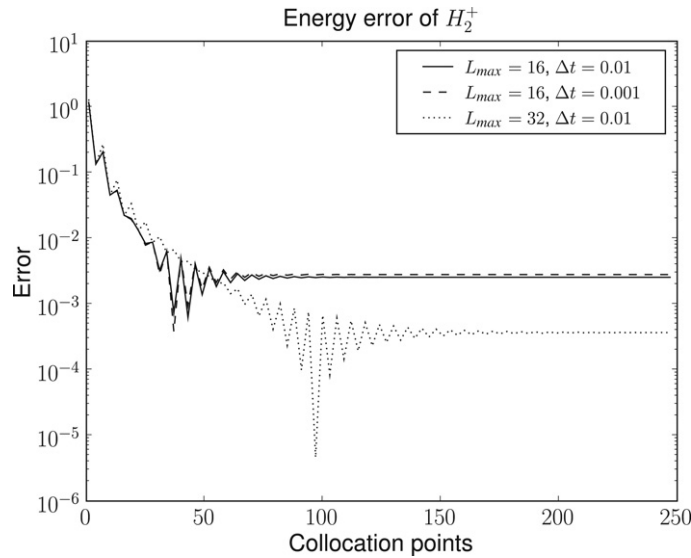


Fig. 7. The error in energy of the ground state of H_2^+ , using transformed Chebyshev basis 1.

It is well known that the ground state energy of a system can be calculated by propagating the system using imaginary time [12]. Furthermore, the ground state energy of H_2^+ can be calculated directly [15], which gives us a basis for comparison.

Clearly, the accuracy of the calculated solution will depend not only on the radial approximation, but also on the time step and the angular discretization (see (12) and (13)). We have therefore run different experiments with different sets of time steps and the number of spherical harmonic basis functions, $S_p = (L_{\max} + 1)^2$.

In Figs. 7 through 10, the error of the calculated ground state energy of H_2^+ is plotted as a function of the number of collocation points. As expected the error, as a function of the number of radial collocation points converges to a non-zero number, determined by the splitting error and/or the angular discretization error.

We notice that the different transformed Chebyshev bases yield rather similar results, while the Fourier basis requires far more basis functions to provide the same accuracy.

Using the Fourier radial basis with $N = 2048$, $L_{\max} = 32$ uses 6.8 sec per time step and requires 132 MB of memory, while the same accuracy can be obtained using only $N = 128$ basis functions in a transformed Chebyshev basis. The reduction in computation is by a factor of 10 while the memory requirement reduces by a factor of 16.

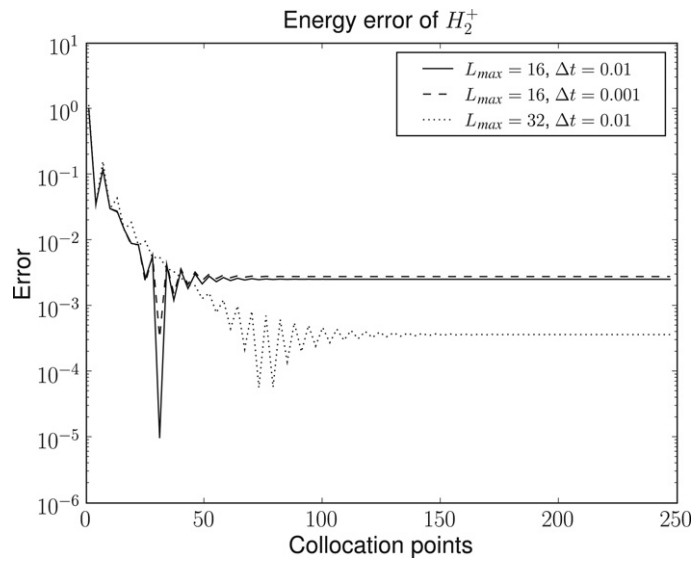


Fig. 8. The error in energy of the ground state of H_2^+ , using transformed Chebyshev basis 2.

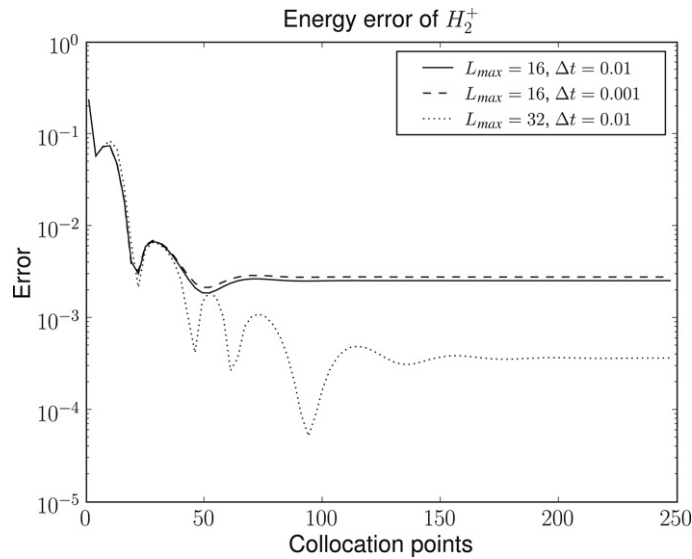


Fig. 9. The error in energy of the ground state of H_2^+ , using transformed Chebyshev basis 3.

6. Conclusions

We have shown that using Chebyshev polynomials as basis functions in combination with a variable transformation may give very accurate spectral approximation of the wavefunction as compared to the Fourier radial basis. In particular, for bounded problems where the wavefunction is located mostly near $r = 0$, the Chebyshev polynomials are superior. However, if the wavefunction is non-stationary and moves to the larger values of r , it enters the domain where the collocation points are distributed sparsely. Consequently, the wavefunction cannot be accurately represented anymore. For these cases, the Fourier basis may be a better choice since it uses an equidistant grid and therefore can provide an equally good resolution through a wide interval of r .

The singular Coulomb potential introduces additional difficulties when split step methods are used. The splitting introduces high frequent oscillations in the intermediate steps which do not disappear after a full time step is completed. One way to deal with this problem is not to do operator splitting, but rather include the potential in the differentiation matrix before finding the eigendecomposition. This can be done because we do not require the basis functions to be eigenfunctions of the operator, as is usually the case when using the Fourier basis. This trick is limited in practice, as one often uses a Kramers–Hennenberger frame [6], or non-symmetric Coulomb potentials as in the H_2^+ -case, which breaks the angular

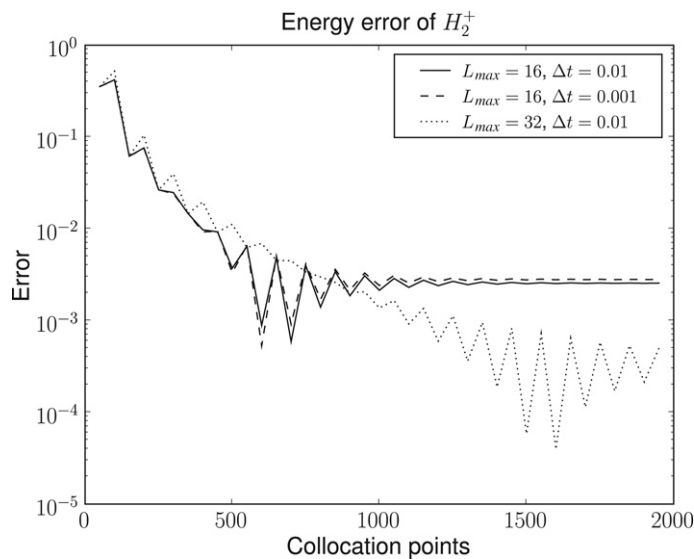


Fig. 10. The error in energy of the ground state of H_2^+ , using the Fourier basis.

symmetry of the Coulomb potential. In this case one needs to consider alternative time stepping schemes, see [9] and references therein.

Acknowledgements

The first and second authors were supported by a grant from the Nanoscience program at the University of Bergen. The third author was supported in part by the VEGA Grant no. 2/7143/27.

References

- [1] John P. Boyd, Chebyshev and Fourier Spectral Methods, Dover Publications, Inc., New York, 2000.
- [2] John P. Boyd, C. Rangan, P.H. Bucksbaum, Pseudospectral method on a semi-infinite interval with application to the hydrogen atom: A comparison of the mapped fourier-sine method with laguerre series and rational chebyshev expansions, *Journal of Computational Physics* 188 (2003) 56–74.
- [3] E. Fattal, R. Baer, R. Kosloff, Phase space approach for optimizing grid representation; The mapped fourier method, *Physical Review E* 53 (1996) 1217.
- [4] M.D. Feit, A. Fleck jr., A. Steiger, Solution of the schrödinger equation by a spectral method, *Journal of Computational Physics* 47 (3) (1982) 412–433.
- [5] Xiaoxu Guan, Xiao-Min Tong, Shih-I Chu, Effect of electron correlation on high-order-harmonic generator of helium atoms in intense laser fields: Time-dependent generalized pseudospectral approach in hyperspherical coordinates, *Physical Review A* 73 (2) (2006).
- [6] Walter C. Henneberger, Perturbation method for atoms in intense light beams, *Physical Review Letters* 21 (12) (1968) 838–841.
- [7] Mark R. Hermann, A. Fleck jr., Split-operator spectral method for solving the time-dependent schrödinger equation in spherical coordinates, *Physical Review A* 38 (12) (1988) 6000–6012.
- [8] Tobias Jahnke, Christian Lubich, Error bounds for exponential operator splitting, *BIT* 40 (4) (2000) 735–744.
- [9] A.K. Kassam, Lloyd Nick Trefethen, Fourth-order time stepping for stiff pdes, *SIAM Journal of Scientific Computing* 26 (4) (2005) 1214–1233.
- [10] Robert I. McLachlan, Reinout W. Quispel, Splitting methods, *Acta Numerica* 11 (2002) 341–434.
- [11] G.M. Muslu, H.A. Erbay, Higher-order split-step fourier schemes for the generalized nonlinear schrödinger equation, *Mathematics and Computers in Simulation* 67 (2005) 581–595.
- [12] Amlan K. Roy, Neetu Gupta, B.M. Deb, Time-dependent quantum-mechanical calculation of ground and excited states of anharmonic and double-well oscillators, *Physical Review A* 65 (1) (2001) 012109.
- [13] Gilbert Strang, On the construction and comparison of difference schemes, *SIAM journal on Numerical Analysis* 5 (1968) 506–517.
- [14] Jingyan Wang, Shih-I Chu, Cecil Laughlin, Multiphoton detachment of h_2 . ii. Intensity photodetachment rates and threshold behavior – complex scaling generalized pseudospectral method, *Physical Review A* 50 (4) (1994) 3208–3215.
- [15] H. Wind, Electron energy for h_2^+ in the ground state, *The Journal of Chemical Physics* 42 (7) (1965) 2371–2373.
- [16] H. Yoshida, Construction of higher order symplectic integrators, *Physics Letters A* 150 (5–7) (1990) 262–268.